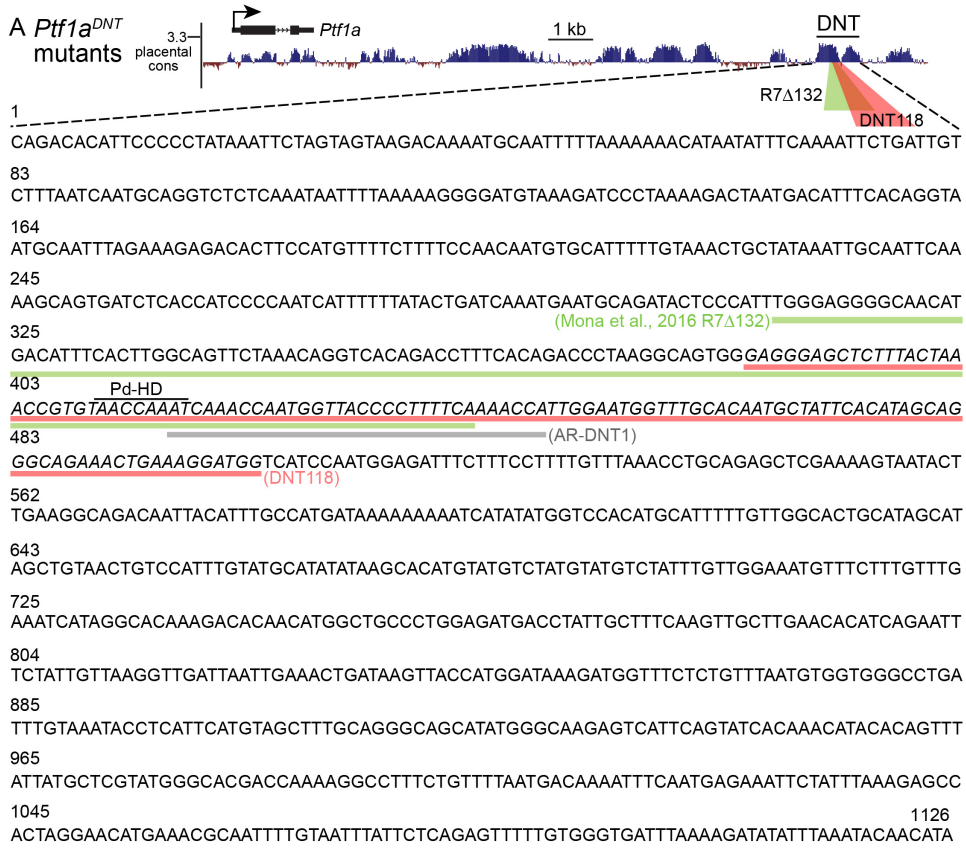
A Ptf1a^DNT mutants
3.3 placental cons
Ptf1a
1 kb
DNT
R7Δ132
DNT118
1
CAGACACATTCCCCCTATAAATTCTAGTAGTAAGACAAAATGCAATTTTTAAAAAAACATAATATTTCAAAATTCTGATTGT
83
CTTTAATCAATGCAGGTCTCTCAAATAATTTTAAAAAGGGGATGTAAAGATCCCTAAAAGACTAATGACATTTCACAGGTA
164
ATGCAATTTAGAAAGAGACACTTCCATGTTTTCTTTTCCAACAATGTGCATTTTTGTAAACTGCTATAAATTGCAATTCAA
245
AAGCAGTGATCTCACCATCCCCAATCATTTTTTATACTGATCAAATGAATGCAGATACTCCCATTTGGGAGGGGCAACAT
(Mona et al., 2016 R7Δ132)
325
GACATTTCACTTGGCAGTTCTAAACAGGTCACAGACCTTTCACAGACCCTAAGGCAGTGGGAGGGAGCTCTTTACTAA
403
Pd-HD
ACCGTGTAACCAAATCAAACCAATGGTTACCCCTTTTCAAAACCATTGGAATGGTTTGCACAATGCTATTCACATAGCAG
483
(AR-DNT1)
GGCAGAAACTGAAAGGATGGTCATCCAATGGAGATTTCTTTCCTTTTGTTTAAACCTGCAGAGCTCGAAAAGTAATACT
(DNT118)
562
TGAAGGCAGACAATTACATTTGCCATGATAAAAAAAAAATCATATATGGTCCACATGCATTTTTGTTGGCACTGCATAGCAT
643
AGCTGTAACTGTCCATTTGTATGCATATATAAGCACATGTATGTCTATGTATGTCTATTTGTTGGAAATGTTTCTTTGTTTG
725
AAATCATAGGCACAAAGACACAACATGGCTGCCCTGGAGATGACCTATTGCTTTCAAGTTGCTTGAACACATCAGAATT
804
TCTATTGTTAAGGTTGATTAATTGAAACTGATAAGTTACCATGGATAAAGATGGTTTCTCTGTTTAATGTGGTGGGCCTGA
885
TTTGTAAATACCTCATTCATGTAGCTTTGCAGGGCAGCATATGGGCAAGAGTCATTCAGTATCACAAACATACACAGTTT
965
ATTATGCTCGTATGGGCACGACCAAAAGGCCTTTCTGTTTTAATGACAAAATTTCAATGAGAAATTCTATTTAAAGAGCC
1045
1126
ACTAGGAACATGAAACGCAATTTTGTAATTTATTCTCAGAGTTTTTGTGGGTGATTTAAAAGATATATTTAAATACAACATA

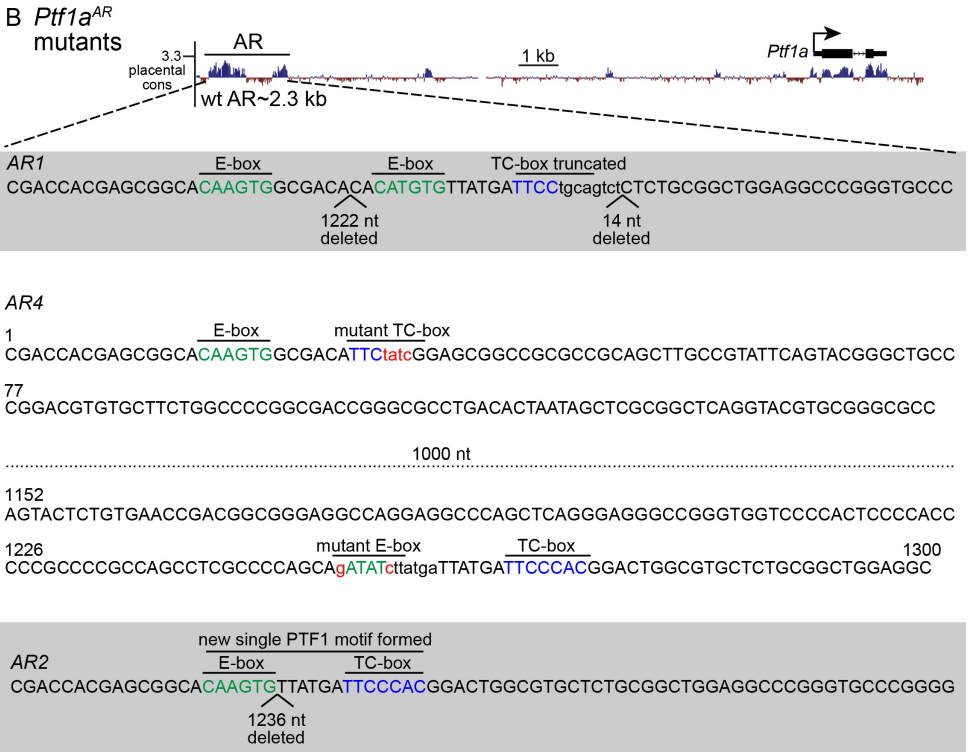
B Ptf1a^AR mutants
3.3 placental cons
AR
wt AR~2.3 kb
1 kb
Ptf1a
AR1
E-box
E-box
TC-box truncated
CGACCACGAGCGGCACAAGTGGCGACACACATGTGTTATGATTCCTgcagtctCTCTGCGGCTGGAGGCCCGGGTGCCC
1222 nt deleted
14 nt deleted
AR4
1
E-box
mutant TC-box
CGACCACGAGCGGCACAAGTGGCGACATTCtatcGGAGCGGCCGCGCCGCAGCTTGCCGTATTCAGTACGGGCTGCC
77
CGGACGTGTGCTTCTGGCCCCGGCGACCGGGCGCCTGACACTAATAGCTCGCGGCTCAGGTACGTGCGGGCGCC
1000 nt
1152
AGTACTCTGTGAACCGACGGCGGGAGGCCAGGAGGCCCAGCTCAGGGAGGGCCGGGTGGTCCCCACTCCCCACC
1226
mutant E-box
TC-box
1300
CCCGCCCCGCCAGCCTCGCCCCAGCAgATATCttatgaTTATGATTCCCACGGACTGGCGTGCTCTGCGGCTGGAGGC
AR2
new single PTF1 motif formed
E-box
TC-box
CGACCACGAGCGGCACAAGTGTTATGATTCCCACGGACTGGCGTGCTCTGCGGCTGGAGGCCCGGGTGCCCGGGG
1236 nt deleted

Supplemental Figure S1 (Related to Figure 1 and Table S1): *Ptf1a* enhancer mutants have disrupted *Ptf1a-DNT* and *Ptf1a-AR* enhancers. (A,B) Genome tracks showing mammalian conservation at the *Ptf1a* locus highlighting the *DNT* (A) and *AR* (B) enhancers with the genotype verified sequence of *Ptf1a*-enhancer mutants generated in this study. (A) The regions within the *DNT* locus deleted in the enhancer mutants *DNT118* and *AR-DNT1* are highlighted in orange and gray, respectively. The region *R7Δ132* tested in Mona et al., 2016 is highlighted in lime green. (B) Mutations and /or deletions in the *AR* enhancer for *AR1*, *AR4* and *AR2* mutant mice are indicated. The entire 2.3 kb enhancer was deleted in *AR-DNT1* (not shown). The PTF1 binding motifs comprising an E-box (green) and a TC-box (blue) are highlighted. Specific mutations in the E-box or TC-box are in red lower case, insertions not found in wildtype sequence is in lower case. (Also see Supplemental Table S1)

Mona el al. Supplemental Fig. S2

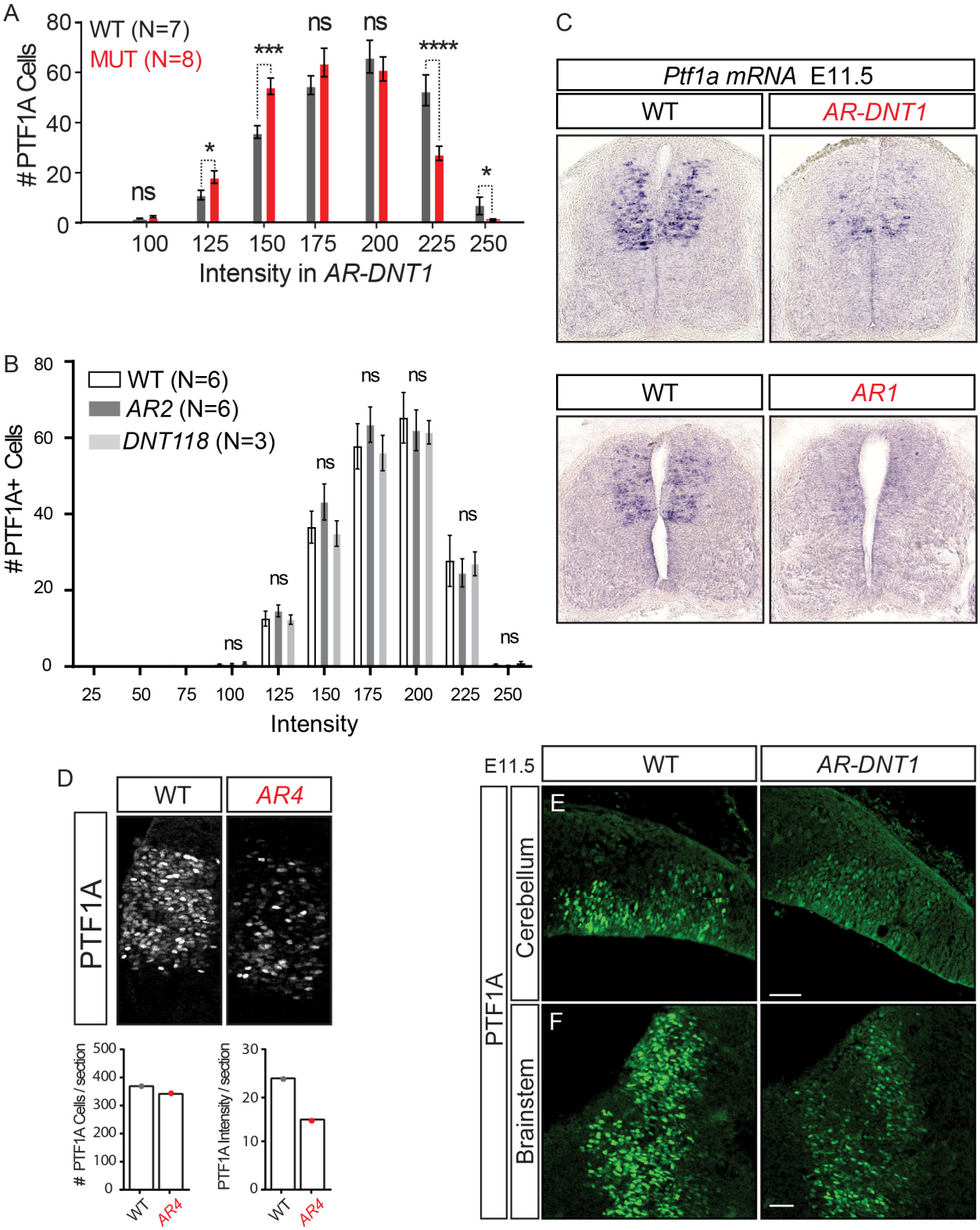

Supplemental Figure S2 (Related to Figure 2): *Ptf1a* enhancer mutants with a scratch phenotype have lower levels of PTF1A relative to mutants with no scratch phenotype. (A,B) Quantification of the number of cells with a particular fluorescence intensity from immunostaining for PTF1A. (A) In *AR-DNT1*, MUT cells have less signal than WT, while in enhancer mutants (B) with no scratch phenotype (*AR2* and *DNT118*), PTF1A levels are similar between MUT and WT littermates. (C) In situ hybridization for *Ptf1a* mRNA in E11.5 mouse neural tube shows reduction in *Ptf1a* mRNA levels similar to what is seen at E10.5 (Fig. 2C) in *AR-DNT1* and *AR1* relative to littermate controls (WT). (D) *AR4* mutant E10.5 neural tube has less PTF1A than WT littermates. (E,F) Immunofluorescence for PTF1A in *AR-DNT1* mutants and littermate controls (WT) in transverse brain sections at E11.5 show reduced levels of PTF1A in the cerebellum (E) and brainstem (F). Error bars indicate SEM. Student's t-test was used to determine significant differences relative to WT, p-values are (*$p<0.05$, ***$p<0.001$, ****$p<0.0001$). Scale bar: 50 μm.

Mona et al. Supplemental Fig. S3

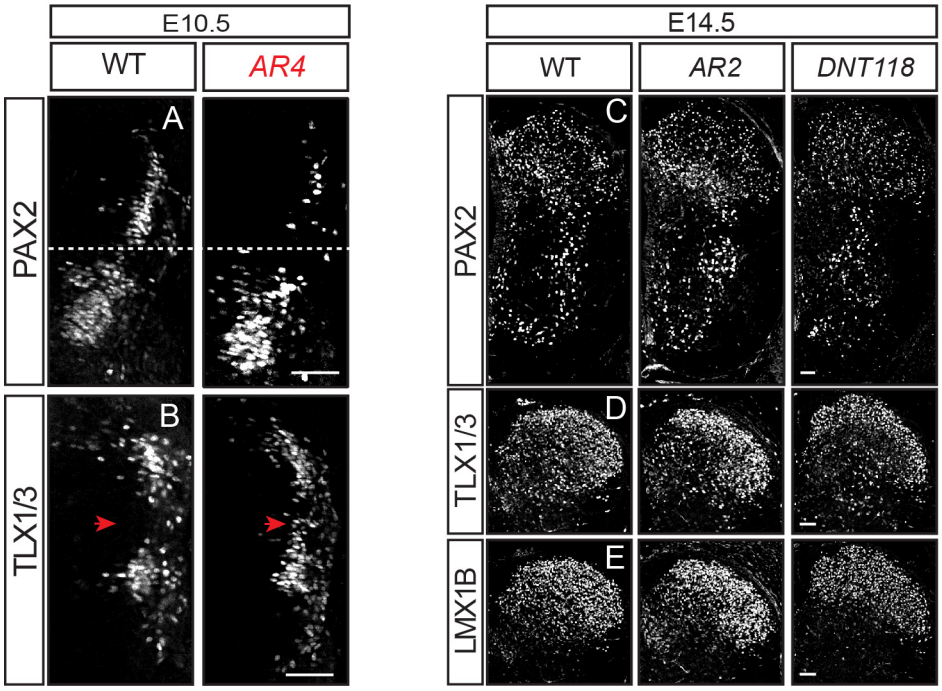

Supplemental Figure S3 (Related to Figure 3): PAX2, TLX1/3 and LMX1B in *Ptf1a* enhancer mutants. (A,B) Immunostaining of PAX2 and TLX1/3 in transverse hemisections of mouse E10.5 neural tube from *AR4* showing a decrease of dorsal PAX2 and an increase in TLX1/3 (red arrowheads) relative to WT. (C-E) Immunostaining for PAX2, TLX1/3, and LMX1B in transverse hemisections of mouse E14.5 neural tube show no change in *AR2* and *DNT118* mutants compared to littermate controls (WT). Scale bar – 50 μm.

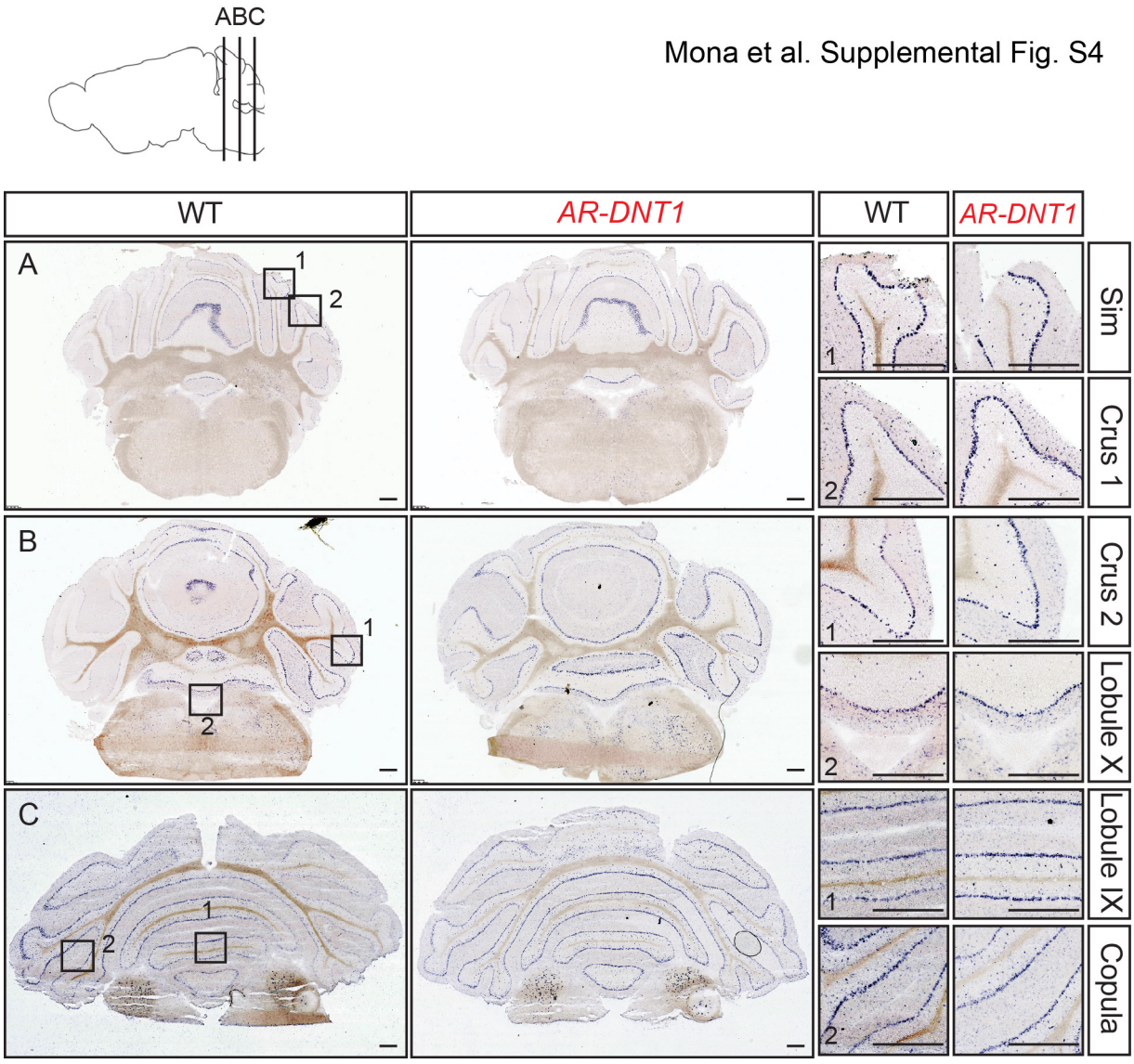

Mona et al. Supplemental Fig. S4

Supplemental Figure S4 (Related to Figure 4): Reduced PTF1A levels do not affect specification of *Gad1+* inhibitory neurons in cerebellum. Sagittal outline of mouse brain locating the coronal section of the cerebellum in A-C. (A,B) In situ hybridization shows no change in *Gad1+* neurons in *AR-DNT1* mutant cerebellum at P30 when compared to WT controls. Black boxes highlight the regions magnified in each section. Regions of the cerebellum highlighted include the simple lobule (Sim), Crus 1, Crus 2, lobules IX and X, and the Copula. Scale bar: 500 μm.

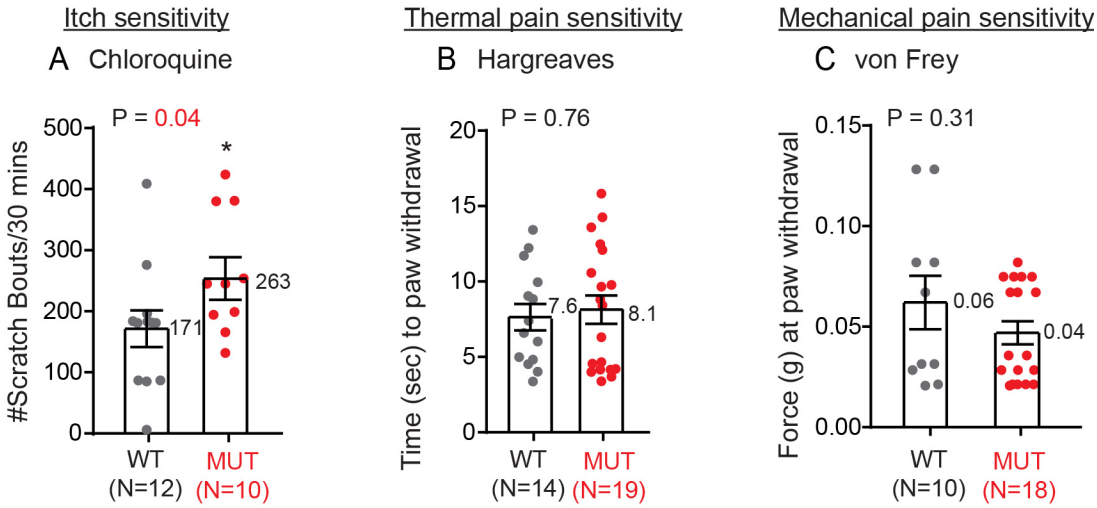

Supplemental Figure S5 (Related to Figure 5): *Ptf1a* enhancer mutants have increased sensitivity to itch inducing pruritogen. (A) Quantification of the number of scratch bouts in 30 minutes after injection of chloroquine at the neck reveals increased sensitivity to itch in the *AR-DNT2* mutants relative to WT similar to *AR-DNT1* (Fig. 5A). (B,C) The Hargreaves thermal sensitivity behavior tests (B) and Von Frey testing for mechanical sensitivity threshold (C) showed no significant difference in the *AR-DNT2* mutants relative to WT littermate controls similar to *AR-DNT1* (Fig. 5C,F). Each data point represents a biological replicate (N); error bars indicate SEM. Student's t-test (See Materials and Methods) was used to determine significant differences relative to WT, p-values are as indicated.

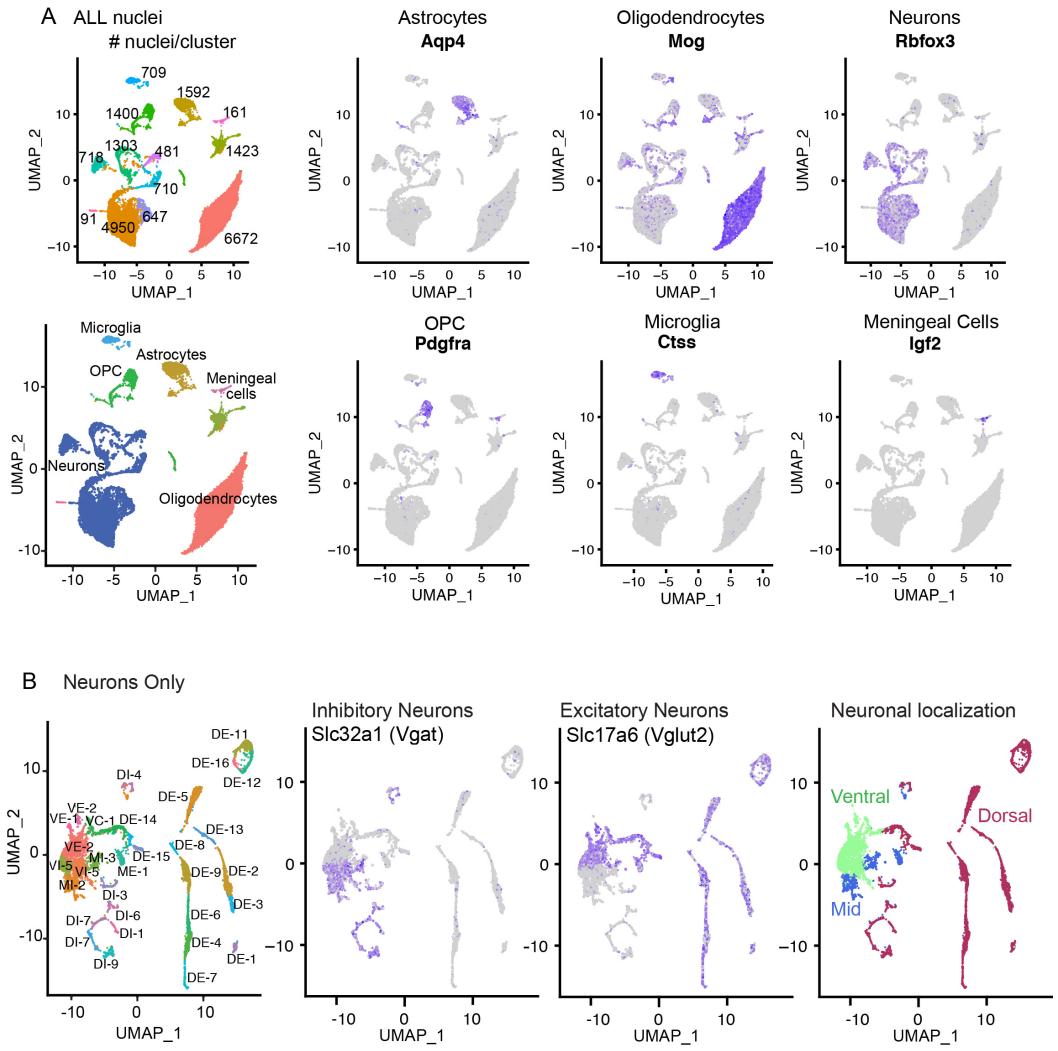

Supplemental Figure S6 (Related to Figure 6): Cervical spinal cord single nuclei RNA-seq cluster analysis. UMAP visualization of the snRNA-seq from P25 cervical spinal cord from *Ptf1a*$^{Cre/AR\text{-}DNT1}$*;Ai14* and *Ptf1a*$^{CRE/+;}$*Ai14* controls combined. (A) 13 clusters were identified and cell-type specific markers were used to assign identity to each cluster as shown. The numbers in the first panel indicate the number of nuclei in that cluster. Representative markers used to define a cell-type are shown on the UMAP graphs. (B) Neurons were re-clustered identifying 31 clusters. These were assigned identities based annotations from Sathyamurthy 2018. *Slc32a1* (*Vgat*) and *Slc17a6* (*Vglut2*) expression are visualized to indicate inhibitory versus excitatory neurons, respectively. The neuronal location as annotated in Sathyamurthy 2018 for ventral, mid, and dorsally localized neurons within the spinal cord is indicated. (also see Materials and Methods, and Supplemental Table S2)

Sathyamurthy, A., Johnson, K.R., Mateson, K.J.E., Dobrott, C.I., Li, L., Ryba, A.R., Bergman, T.B., Kelly, M.C., Kelley, M.W. and Levine, A.J. (2018) Massively Parallel Single Nucleus Transcriptional Profiling Defines Spinal Cord Neurons and Their Activity During Behavior. Cell Rep *22*, 2216-2225